Molecular and Cellular Proteomics

Copy of e-mail notification zjw4257

MCP proofs: M111.015768 article 4257 ready for download

_____

Dear Dr. Guthals:

Email Address: your e-mail address
Password: QtEgYYN2o3og

To view your Molecular and Cellular Proteomics article, please refer to this URL address
http://rapidproof.cadmus.com/RapidProof/retrieval/index.jsp

You will need to have Adobe Acrobat Reader software to read these files. This is free software and is available for user downloading at http://www.adobe.com/products/acrobat/readstep.html.

Our NEW INVOICING/ORDERING SYSTEM is now available online. Shortly you will be receiving a separate e-mail message that contains the link related to this article.

Proof corrections may be returned in several ways:

You may print the PDF file (use normal quality), hand-mark your corrections, and scan the corrected proofs and all forms as a PDF to return as an e-mail attachment.

Proof corrections will also be accepted in annotated PDF format. You must have the full version of Adobe Acrobat not just Reader to annotate the PDFs. PLEASE DO NOT USE YELLOW BALLOONS, STICKY NOTES, OR BLUE CARETS. Go to the Tools menu and select "Commenting" or "Drawing markups." We are only able to process the annotated PDFs if you follow these steps:

1) Indicate deletions in text by highlighting the area and using the Cross-out text tool.
2) Use the Pencil tool to also indicate deletions in the margin with the proofreading symbol.
3) Insert new text using the Call-out tool icon.
4) Resize and move the text box so that it appears in white space and does not cover any correction.

OR, if you prefer, you may print the PDF file (use normal quality), hand-mark your corrections using blue ink, and return them via overnight mail.
Please read the page proofs carefully and
1) indicate changes or corrections in the margin of the page proofs;
2) answer all queries (footnotes A,B,C, etc.) on the query sheet;
3) proofread any tables and equations carefully;
4) check that any Greek, especially mu, has translated correctly.
5) please check all color figures and note clearly any concerns about color reproduction.

Within 48 hours we will need:
1) Original PDF set of page proofs including query sheet with answers.
2) IF figure corrections are needed, please send a TIFF, EPS, or PDF of the corrected figure as an attachment to e-mail (use RGB for color).
3) Notice to Author form (cannot publish without this).
4) Signed Copyright Assignment form (cannot publish without this)

PLEASE INCLUDE YOUR ARTICLE NO. (4257) WITH ALL CORRESPONDENCE.

Attn: Isabel Castillo

Molecular & Cellular Proteomics
5457 Twin Knolls Road., Suite 200
Columbia, MD 21045 USA
castilloi@cadmus.com
Tel: 1-410-691-6454
Fax: 1-410-684-2790

Proofreader's Marks

MARK	EXPLANATION	EXAMPLE
	TAKE OUT CHARACTER INDICATED	 Your proof.
	LEFT OUT, INSERT	 Your proof.
	INSERT SPACE	 Yourproof.
	TURN INVERTED LETTER	Your proof.
	BROKEN LETTER	Your proof.
	EVEN SPACE	A good proof.
	CLOSE UP: NO SPACE	Your proof.
	TRANSPOSE	A proof good
	WRONG FONT	 Your proof.
	LOWER CASE	Your proof.
	CAPITALS	Your proof.  Your proof.
	ITALIC	Your proof. Your proof.
	ROMAN, NON ITALIC	 Your proof.
	BOLD FACE	Your proof. Your proof.
	LET IT STAND	Your proof.  Your proof.
	DELETE, SEE COPY	She Our proof.
	SPELL OUT	 Queen Eliz.
	START PARAGRAPH	 read. Your
	NO PARAGRAPH: RUN IN	marked. Your proof.
	LOWER	 Your proof.

MARK	EXPLANATION	EXAMPLE
	RAISE	 Your proof.
	MOVE LEFT	Your proof.
	MOVE RIGHT	Your proof.
	ALIGN TYPE	Three dogs. Two horses.
	STRAIGHTEN LINE	Your proof.
	INSERT PERIOD	Your proof
	INSERT COMMA	Your proof
	INSERT COLON	Your proof
	INSERT SEMICOLON	Your proof
	INSERT APOSTROPHE	Your mans proof.
	INSERT QUOTATION MARKS	Marked it proof
	INSERT HYPHEN	A proofmark.
	INSERT EXCLAMATION MARK	Prove it
	INSERT QUESTION MARK	Is it right
	QUERY FOR AUTHOR	Your proof read by
	INSERT BRACKETS	The Smith girl
	INSERT PARENTHESES	Your proof 1
	INSERT 1-EM DASH	Your proof.
	INDENT 1 EM	Your proof
	INDENT 2 EMS	Your proof.
	INDENT 3 EMS	Your proof.

NOTICE TO AUTHORS

To avoid delay in publication, please provide complete information to the following questions.

Author's Choice (choice must match pro forma invoice line)

☐ I want full access to my article available immediately in PubMed.
- ☐ Member of ASBMB ($1500 fee)
- ☐ Non-member of ASBMB ($2000 fee)

■ I do not want to pay extra for immediate access to my article.

Revised Page Proofs

Revised page proofs can be sent electronically to you if you have a specific concern regarding the makeup of your paper or if there are extensive alterations. Please note that revised page proofs are used for confirmation purposes only and are not considered as a second opportunity for corrections.

■ I do not need revised page proofs. Please expedite publication after incorporating any changes I have indicated.

☐ Please send revised page proofs. Revised page proofs are an opportunity for you to check typographical errors in your alterations, and not to make any additional corrections.

PLEASE SIGN COPYRIGHT NOTICE.
PLEASE RETURN PAGE PROOFS AND ALL OTHER CORRESPONDENCE WITHIN 48 HOURS.

To pay your fees, please look for an e-mail that contains the link to the new online payment and reprints ordering system

THANK YOU.

Molecular & Cellular Proteomics

Cadmus Professional Communications
8621 Robert Fulton Dr., Suite 100
Columbia, MD 21046

RE: _____

-- COPYRIGHT ASSIGNMENT –

Papers cannot be published unless a signature is on file.

Please return this form with your page proofs.

To: American Society for Biochemistry and Molecular Biology, Inc. (ASBMB)

I/We hereby confirm that

a) The ASBMB shall, in consideration of publication, become entitled to the work copyright and translation rights therein and that I/we assign all copyrights in the paper to ASBMB for publication in printed and electronic forms.

b) For U.S. Government Employees: This work was done in my capacity as an U.S. government employee; the above assignment applies only to the extent allowable by law.

Signed: All authors shall sign, or the signing author must indicate that consent is held from each co-author for copyright to be assigned to ASBMB.

Date: _____

Signed: _____

■ I hold consent from each co-author for copyright to be assigned to ASBMB.

Molecular & Cellular Proteomics

Cadmus Professional Communications
Airport Square Building 7
8621 Robert Fulton Dr., Suite 100
Columbia, MD 21046

COLOR ARTICLES ONLY

We CANNOT publish your article until we receive approval of the reproduction quality for your color figure(s). Please view your color images on the computer screen and fax or e-mail your approval to me within 24 hours, referring to the article number.

Thank you,

Isabel Castillo

Molecular & Cellular Proteomics
8621 Robert Fulton Dr., Suite 100
Columbia, MD 21046
Tel: 410-691-6256
Fax: 410-684-2790
E-mail: castilloi@cadmus.com

P.S. When you return the page proofs, please be sure to indicate the total number of reprints desired. It is also important to return your reprint order form as quickly as possible to make sure the color reprints are ordered promptly.

Shotgun Protein Sequencing With Meta-contig Assembly*[S]

Adrian Guthals‡‖, Karl R. Clauser¶, and Nuno Bandeira‡§

Full-length *de novo* sequencing from tandem mass (MS/MS) spectra of unknown proteins such as antibodies or proteins from organisms with unsequenced genomes remains a challenging open problem. Conventional algorithms designed to individually sequence each MS/MS spectrum are limited by incomplete peptide fragmentation or low signal to noise ratios and tend to result in short *de novo* sequences at low sequencing accuracy. Our shotgun protein sequencing (SPS) approach was developed to ameliorate these limitations by first finding groups of unidentified spectra from the same peptides (contigs) and then deriving a consensus *de novo* sequence for each assembled set of spectra (contig sequences). But whereas SPS enables much more accurate reconstruction of *de novo* sequences longer than can be recovered from individual MS/MS spectra, it still requires error-tolerant matching to homologous proteins to group smaller contig sequences into full-length protein sequences, thus limiting its effectiveness on sequences from poorly annotated proteins. Using low and high resolution CID and high resolution HCD MS/MS spectra, we address this limitation with a Meta-SPS algorithm designed to overlap and further assemble SPS contigs into Meta-SPS *de novo* contig sequences extending as long as 100 amino acids at over 97% accuracy without requiring any knowledge of homologous protein sequences. We demonstrate Meta-SPS using distinct MS/MS data sets obtained with separate enzymatic digestions and discuss how the remaining *de novo* sequencing limitations relate to MS/MS acquisition settings. *Molecular & Cellular Proteomics 11: 10.1074/mcp.M111.015768, 1–13, 2012.*

Database search tools, such as Sequest (3), Mascot (4), and InsPecT (5), are the most frequently used methods for reliable protein identification in tandem mass (MS/MS) spectrometry based proteomics. These operate by separately matching each MS/MS spectrum to peptide sequences from reference protein databases where all proteins of interest are presumably contained. But this assumption often does not hold true as many important proteins, such as monoclonal antibodies, are not contained in any database because mechanisms of antibody variation (including genetic recombination and somatic hypermutation (6)) constantly create new proteins with novel unique sequences. These mechanisms of variation are the foundation of adaptive immune systems and have enabled highly successful antibody-based therapeutic strategies (7, 8). Nevertheless, such variation also means that antibody MS/MS spectra are typically impossible to identify via standard database search techniques whenever the corresponding sequences are not known in advance. An inherent drawback of database search strategies is that they are only as good as the database(s) being searched and incomplete databases often result in proteins being misidentified or left unidentified (9).

Despite the importance of novel protein identification, few high-throughput methods have been developed for *de novo* sequencing of unknown proteins. Low-throughput Edman degradation is a well-known *de novo* sequencing approach that can accurately call amino acid sequences in N/C-terminal regions of unknown proteins but has drawbacks that make it unsuitable for sequencing proteins longer than 50 amino acids or proteins with post-translational modifications (10, 11). Many have recognized the potential of tandem mass spectrometry for protein sequencing. For example, in 1987 Johnson and Biemann (12) manually sequenced a complete protein from rabbit bone marrow. Meanwhile, automated *de novo* sequencing methods that rely on interpretations of *individual* MS/MS spectra are limited in that they typically cannot reconstruct long (8+ AA) sequences without mis-predicting 1 in 5 AA on average for low accuracy collision-induced dissociation (CID) spectra (13, 14). Recent advances in *de novo* peptide sequencing have improved sequencing accuracy to over 95% for high resolution higher energy collisional dissociation (HCD)[1] spectra (15), but at lim- Fn1

From the ‡Department of Computer Science and Engineering, §Skaggs School of Pharmacy and Pharmaceutical Sciences, University of California San Diego, La Jolla, California 92093; ¶Broad Institute of the Massachusetts Institute of Technology and Harvard, Cambridge, Massachusetts 02142

Received November 11, 2011, and in revised form, June 5, 2012
Published, MCP Papers in Press, July 13, 2012, DOI 10.1074/mcp.M111.015768

[1] The abbreviations used are: HCD, higher-energy collisional dissociation; SPS, Shotgun Protein Sequencing approach to de novo protein sequencing (1); cSPS, Comparative Shotgun Protein Sequencing approach (2); Meta-SPS, SPS with assembly of contigs into meta-contigs (described here); PTM, post-translational modification; ETD, electron transfer dissociation; PRM, prefix-residue mass; SRM, suffix-residue mass; FDR, false discovery rate; MS/MS, tandem mass spectrometry; LC, liquid chromatography; aBTLA, antibody raised against the B- and T- lymphocyte attenuator molecule (described in (2)); 6-prot, mixture of six proteins: bovine purified from lung, recombinant murine leptin expressed in E. coli, horse heart myoglobin purified from heart, horseradish purified from horseradish roots, E. coli GroEL purified from an E. coli strain overexpressing GroEL, and human prostate-specific antigen (also known as kallikrein-related peptidase) purified from seminal fluid.

ited sequence coverage (Chi H *et al.* report only 55% sequence coverage of peptides identified by database search). In fact, all current per-spectrum *de novo* sequencing strategies face a significant tradeoff between sequencing accuracy and coverage as spectra exhibiting complete peptide fragmentation rarely cover entire target proteins, yet are required to accurately reconstruct full-length peptide sequences. An alternative approach to separately sequencing individual spectra is to *simultaneously* interpret *multiple* MS/MS spectra from overlapping peptides. This Shotgun Protein Sequencing (SPS) paradigm differs from traditional algorithms by deriving consensus sequences from *contigs* - sets of multiple MS/MS spectra from distinct peptides with overlapping sequences (1, 16). Because SPS aggregates multiple spectra from overlapping peptides, protein sequences extending beyond the length of enzymatically digested peptides can be extracted from spectra with incomplete peptide fragmentation. Furthermore, SPS has been found to generate sequences that frequently cover 90–95+% of the target protein sequence(s) whereas mis-predicting only 1 out of every 20 amino acids on high resolution MS/MS spectra (2). But a remaining limitation of SPS is that it still generates fragmented sequences that do not singularly cover large regions of the target protein sequences, much less complete proteins: SPS sequences have an average length of 10–15 amino acids (depending on input data) and the longest recovered SPS *de novo* sequence is less than 45 amino acids long (1).

The considerable limitations of *de novo* sequencing strategies have typically been addressed by attempting to circumvent them using error-tolerant matching to known protein sequences. One such strategy (17) is to generate short *de novo* sequence tags and then match them exactly to protein databases without requiring matching the N/C-term flanking masses (to allow for unexpected polymorphisms or post-translational modifications). Short sequence tags are usually derived from parts of the spectrum with high signal-to-noise ratios and typically have higher sequencing accuracy than full-length *de novo* sequences (18). This approach was later extended in MS-Shotgun (19) and continues to be a popular technique for speeding up database search tools (5, 20–22). Homology matching of full length *de novo* sequences was first explored in CIDentify (23) and later in MS-BLAST (24) by searching *de novo* sequences using FASTA and WU-BLAST2 (respectively) to find homologous matches to sequences of related proteins; FASTS (25) also approached the problem using a modified version of FASTA. However, common *de novo* sequencing errors tend to produce sequences that are heavily penalized in pure sequence homology searches. For example, missing peaks in MS/MS spectra may easily cause GA subsequences to be reconstructed as Q or AG (same-mass sequences), thus making subsequent BLAST searches unlikely to succeed. This issue was partially considered in CIDentify and more thoroughly addressed in SPIDER (26) by explicitly modeling *de novo* sequencing errors together with BLOSUM scores in MS/MS-based sequence homology searches. In addition, OpenSea (27) further explored database matching of *de novo* sequences for analysis of unexpected post-translational modifications (PTMs). Finally, Shen *et al.* (28) used short unique *de novo* sequence tags, called UStags, to discover protein-localized PTMs.

Recent approaches to homology matching of *de novo* sequences have built on genome assembly and sequencing techniques to achieve database-assisted full-length sequencing of unknown proteins. Comparative Shotgun Protein Sequencing (cSPS) complemented SPS assembly techniques with usage of error tolerant matching of *de novo* sequences to find overlapping SPS *de novo* sequences that are then further assembled into full-length protein sequences (2). cSPS was designed to support the sequencing of highly divergent proteins that have regions close enough in homology to transfer matches from a reference. cSPS was shown to enable *de novo* sequencing of monoclonal antibodies at 95+% sequencing accuracy, while simultaneously tolerating and identifying unexpected PTMs (29). In difference from cSPS, Champs (30) *de novo* sequences individual spectra to obtain putative peptide sequences, which are then mapped to homologous proteins to correct sequencing errors and reconstruct protein sequences with 100% accuracy and 99% coverage. However, Champs is designed to only map peptides that differ from the reference sequence by one or two amino acids and does not handle PTMs. As such, its sequencing accuracy is not directly comparable to that of cSPS as Champs was not designed to sequence highly divergent proteins (such as monoclonal antibodies) with multiple PTMs, insertions, deletions, and/or recombinations. GenoMS (31) extended the approaches in cSPS/Champs by explicitly modeling protein splice variants as paths in splice graphs where nodes represent translated exon regions (32). MS/MS spectra are first searched for exact sequence matches against all possible protein isoforms. The remaining unidentified MS/MS spectra are then aligned to the matched peptides and *de novo* sequenced to extend the matched sequences into novel regions. Reported sequences are 97–99% accurate and cover 96–99% of target proteins depending on sequence similarity between the novel and reference sequences (31). However, GenoMS *de novo* sequences are usually extended less than 3 amino acids beyond matched peptides because sequencing accuracy degrades as sequences are extended, thus preventing the consistent extension of long (10+ AA) sequences. Altogether, the use of homology matching approaches for full-length *de novo* protein sequencing continues to be limited by 1) requiring the previous knowledge of closely related protein sequences and 2) the inherent difficulties in statistically significant homology-tolerant matching of error-prone short *de novo* sequences.

The Meta-SPS approach proposed here seeks to *de novo* sequence complete proteins, or long protein regions, without *any* use of a database. Meta-SPS builds upon SPS by treating

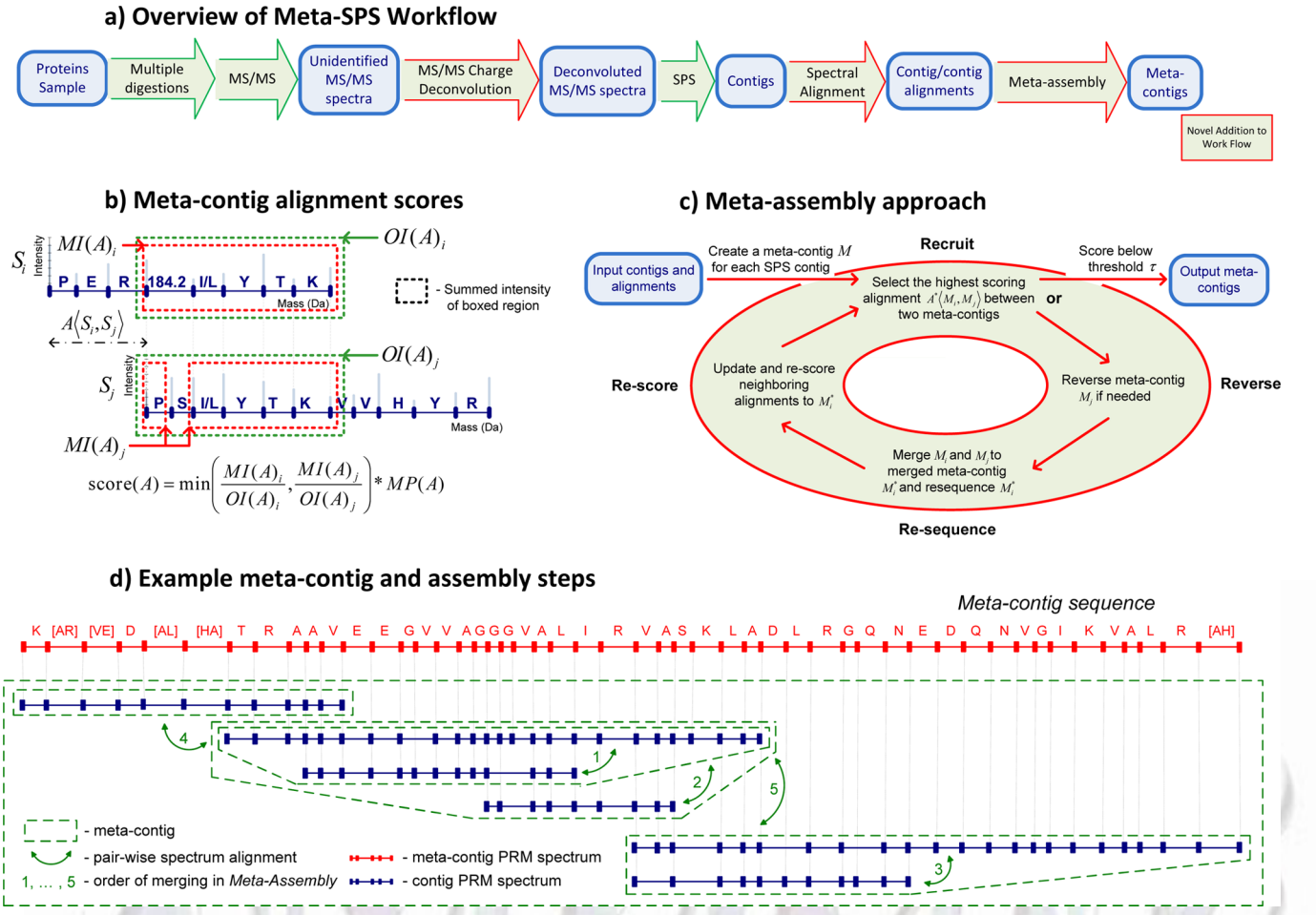

FIG. 1. **Meta-SPS Procedures.** *A*, *Green* arrows denote procedures previously described in (1) and *red* arrows denote procedures described here. The SPS step involves spectral clustering by MSCluster (34), PepNovo+ PRM scoring (35), and assembly of mass spectra into contigs (1). *B*, An alignment between two PRM spectra is represented as the shift of the second spectrum wrt the first that yields the highest possible score. The displayed scoring function takes the minimum matched/overlapping intensity ratio and multiplies by the number of matching peaks (denoted by *MP*(*A*) for alignment $A\langle S_i,S_j\rangle$ between contig PRM spectra S_i and S_j). Matched and overlapping intensities for each spectrum are displayed as *red* and *blue* boxed regions, respectively. Sequences are not known in advance; shown only for illustration purposes. *C*, Here aligned SPS contigs are assembled into meta-contigs by iteratively merging the highest scoring alignment until remaining alignments have a low score. By merging the highest scoring alignment at every iteration, it is guaranteed that all inconsistent alignments that were removed have a lower score. *D*, *Green* arrows denote merged alignments and numbers correspond to the order in which they alignments are merged. Initially, every contig was in its own meta-contig. The 6 meta-contigs were then merged by five alignments, yielding a single meta-contig PRM spectrum and its meta-contig sequence.

SPS *de novo* sequences (*contig sequences*) as input spectra and further assembling them into longer *de novo* sequences (*meta-contig sequences*). We show that Meta-SPS extends *de novo* sequences to lengths over 100 AA while boosting sequencing accuracy to only 1 mistake per 40 amino acid predictions, thus enabling database-free *de novo* sequencing of completely novel proteins while also allowing error-tolerant matching approaches to support higher-divergence homologies (by searching longer, more accurate *de novo* sequences). Meta-SPS algorithms are demonstrated on CID and HCD MS/MS spectra and its limitations are discussed in relation to the underlying limitations of bottom-up tandem mass spectrometry.

EXPERIMENTAL PROCEDURES

The Meta-SPS workflow is illustrated in Fig. 1*A*. In brief, because Meta-SPS relies upon the interpretation of MS/MS spectra from overlapping peptides, sample proteins were digested with multiple enzymes. Following MS/MS acquisition, *MS/MS Charge Deconvolution* was performed to convert all MS/MS fragment peaks to charge one (see supplemental Materials - MS/MS Charge Deconvolution) and Shotgun Protein Sequencing (SPS) (1) was used to assemble unidentified MS/MS spectra into contigs—sets of aligned spectra from peptides with overlapping sequences. SPS contigs were then aligned to each other using *Spectral Alignment* and further assembled into meta-contig sequences in the *Meta-Assembly* step. Two data sets were used to develop and benchmark Meta-SPS: a mixture of 6 known proteins (6-prot) and a previously described data set from a purified monoclonal antibody raised against the B- and T- lymphocyte

F1,AQ:A

ZSI

attenuator molecule (aBTLA) (2). Briefly, the aBTLA data set consisted of 44,985 MS/MS spectra from the heavy chain and 39,135 MS/MS spectra from the light chain acquired on a Thermo LTQ XL instrument either in the Linear trap (low MS/MS mass accuracy) or in the Orbitrap (high MS/MS mass accuracy). Heavy-chain samples were prepared using five different protease digestions (trypsin, chymotrypsin, pepsin, Glu-C, and AspN) and light-chain samples were prepared with four different protease digestions (trypsin, chymotrypsin, pepsin, and AspN).

6-prot Data Acquisition—For the 6-prot sample, first an equimolar mixture of six proteins was prepared. After reduction and alkylation of cysteines, aliquots were digested by different means to produce sets of overlapping peptides. Bovine (6.5 kDa, catalog # A-4529) purified from lung, recombinant murine leptin (16 kDa, catalog # L-3772) expressed in *E. coli*, horse heart myoglobin (17 kDa, catalog # M-1882) purified from heart, and horseradish peroxidase (39 kDa, catalog # P-6782) purified from horseradish roots were purchased from Sigma-Aldrich. *E. coli* GroEL (57 kDa, catalog # G8976) purified from an *E. coli* strain overexpressing GroEL was purchased from United States Biological (Swampscott, MA). Human prostate-specific antigen also known as kallikrein-related peptidase (29 kDa, catalog # P0725) purified from seminal fluid was purchased from Scripps Laboratories (San Diego, CA). The 252 μg total protein mixture was prepared in 100 mM NH_4HCO_3 then reduced with 5 mM dithiothreitol, and the cysteines were alkylated with 20 mM iodoacetamide. The proteins that had not already precipitated were further precipitated with 60% ice-cold ethanol. After centrifugation, the supernatant was removed and discarded. The pellet was washed several times with 95% cold ethanol and then resuspended in 0.04% Rapigest (Waters Corp. Milford, MA) an acid-labile SDS-like detergent. Seven 32 μg aliquots were created. Three aliquots were diluted to 0.085% Rapigest at pH 8.0 in 100 mM NH_4HCO_3 and digested for 6 h. with trypsin 1:150, Lys-C 1:300, or Glu-C 1:150. Three aliquots were diluted to 0.01% Rapigest at pH 8.0 in 100 mM NH_4HCO_3 and digested for 6 h. with Asp-N 1:300, Chymotrypsin 1:150, or Arg-C 1:150. Digestions were stopped, and the detergent was cleaved by acidifying with 1% trifluoro acetic acid (TFA), pH 2. The 7th aliquot was acidified and precipitated with 60% ice-cold ethanol, washed with 95% cold ethanol, dried and digested with cyanogen bromide (CNBr) using 70% TFA for 36 h before drying in a SpeedVac and resuspending in 0.1% TFA. Digests were stored at −80′C prior to LC-MS/MS.

Digests were analyzed with an automated nano LC-MS/MS system, consisting of an Agilent 1100 nano-LC system (Agilent Technologies, Wilmington, DE) coupled to an LTQ-Orbitrap Fourier transform mass spectrometer (Thermo Fisher Scientific, San Jose, CA) equipped with a nanoflow ionization source (James A. Hill Instrument Services, Arlington, MA). Peptides were eluted from a 10 cm column (Picofrit 75 μm ID, New Objectives) packed in-house with ReproSil-Pur C18-AQ 3 μm reversed phase resin (Dr. Maisch, Ammerbuch Germany) using a 95 min acetonitrile/0.1% formic acid gradient at a flow rate of 200 nl/min to yield ~20 s peak widths. Solvent A was 0.1% formic acid and solvent B was 90% acetonitrile/0.1% formic acid. The elution portion of the LC gradient was 3–7% solvent B in 1 min, 67–37% in 60 min, 37–90% in 6 min, and held at 90% solvent B for 5 min. Data-dependent LC-MS/MS spectra were acquired in ~3 s cycles; each cycle was of the following form: one full Orbitrap MS scan at 60,000 resolution followed by five MS/MS scans in the orbitrap at 7,500 or 15,000 resolution on the most abundant precursor ions using an isolation width of 2.0 or 2.5 *m/z*. Dynamic exclusion was enabled with a mass width of ± 25 ppm, a repeat count of 1 and an exclusion duration of 8 s. Charge state screening was enabled along with monoisotopic precursor selection and nonpeptide monoisotopic recognition to prevent triggering of MS/MS on precursor ions with unassigned charge or a charge state of 1. For CID fragmentation the normalized collision energy was set to 30 with an activation Q of 0.25 and activation time of 30 ms. For HCD fragmentation the normalized collision energy was set to 60 (first generation, "software HCD" with 1 segment of black restrictor capillary tubing removed to elevate the ion gauge operating pressure to 1.6 e-5 Torr).

Spectrum Preprocessing and Notation—A total of 11010 high resolution CID and 14040 high resolution HCD 6-prot spectra were obtained after quality filtering by SpectrumMill. All 6-prot spectra were then deconvoluted using MS/MS Charge Deconvolution (see supplemental Materials) and searched with MS-GFDB (33) against the six target proteins and known contaminants with a spectrum-level false discovery rate of 1%; resulting peptide IDs covered 87% of the target proteins. See supplemental Materials for parameters used for SpectrumMill, MS/MS Charge Deconvolution, and MS-GFDB. ZSI ZSI

High resolution aBTLA MS/MS spectra were also deconvoluted using our approach and repeated spectra were detected and converted to consensus spectra using MS-Cluster (34) separately for low and high resolution spectra. This resulted in 8328 high resolution and 13,863 low resolution clustered CID spectra from the aBTLA light chain, as well as 13,261 high resolution and 14,424 low resolution clustered CID spectra form the aBTLA heavy chain. Spectra were then searched using MS-GFDB at 1% spectrum-level FDR and the resulting peptide identifications covered 99% of the aBTLA protein sequence. We note that peptide identifications were only used for benchmarking the accuracy and coverage of *de novo* sequences. The following notation is used below: a peptide MS/MS spectrum S is defined as a collection of peaks where each peak $p \in S$ corresponds to an ion with mass m[p], charge z[p], intensity i[p], and where p = m[p]/z[p]. The parent mass P[S] is the cumulative mass of all residues in the peptide sequence plus the mass of H_2O and the precursor charge Z[S] is the charge of the peptide ion.

Shotgun Protein Sequencing—SPS uses MS-Cluster (34) to cluster deconvoluted spectra from the same peptide and uses PepNovo$^+$ (35) to convert clustered MS/MS spectra into PRM (prefix residue mass) spectra where peak intensities are replaced with log-likelihood scores. Ideal PRM spectra have peaks only at prefix residue masses (PRMs, cumulative amino acid masses of N-term prefixes of the peptide sequence) and peak scores combining evidence supporting the presence of b/y-ions, such as peak intensity, neutral losses (*e.g.* loss of H_2O) and b/y-ion complementarities, and contrasting it with the estimated level of noise (13, 36). But in actuality, PRM scoring procedures cannot perfectly differentiate between prefix residue masses and suffix residue masses (SRMs, cumulative amino acid masses of C-term suffixes of the peptide sequence plus the mass of H_2O) when complementary b and y ion series are present in a spectrum. PRM and SRM peaks typically receive high scores relative to other peaks whereas PRM peaks usually explain a higher percentage of a spectrum's total score.

SPS then aligns PRM spectra to each other in an all-to-all comparison. For each pair of overlapped spectra, PRM and SRM peaks are separated by two complementary alignments, which can be visualized as complementary paths in an alignment matrix (supplemental Fig. S1). PRM spectrum alignments are retained if their scores are above a certain threshold: SPS fits a Gaussian distribution to spectra alignment scores and chooses score thresholds corresponding to a given p value (0.045); an alignment between two spectra is retained if it passes the significance threshold for both aligned spectra. Because MS/MS spectra from different acquisition modes have different ion statistics, PRM spectra from different acquisition modes were run separately through SPS. Because the alignments are symmetric because of the b/y-ion and PRM/SRM complementarities, SPS cannot tell which peaks are PRMs and which peaks are SRMs, only differentiate between the two. Therefore, contig sequences can assemble ZSI

either aligned PRM peaks or aligned SRM peaks with the majority (~70%) of sequences assembling PRM peaks as they typically receive higher scores than SRM peaks (1). Contig sequences assembling SRM peaks must be reversed to match the target protein sequence in the correct orientation.

Finally, SPS assembles aligned PRM spectra into *contigs*, which are sets of aligned spectra from overlapping peptides (1). Each contig has a corresponding *de novo contig sequence*, which is the sequence of amino acids and mass gaps (masses that do not match the mass of a single amino acid) that best explains the overlapping peaks in the assembled spectra (supplemental Fig. S1). Each contig sequence returned by SPS is represented as a *contig PRM spectrum*, which is a spectrum S with PM[S] equal to the cumulative mass of all residues and gaps in the contig sequence. Each prefix of the contig sequence corresponds to a contig PRM peak and the score of each contig PRM is the summed score of its assembled spectrum PRMs.

Spectral Alignment—Overlaps between contig PRM spectra were computed using a modified version of the spectral alignment technique introduced in SPS (16). An alignment between two PRM spectra S_i and S_j is a set of matched PRM pairs imposed by the shift $A\langle S_i,S_j\rangle$ (defined below) such that for each matched PRM pair (p_i,p_j), $p_i \in S_i$, $p_j \in S_j$, and $p_i = p_j + A\langle S_i,S_j\rangle$. Because some contig sequences may be reversed wrt each other, the highest scoring alignment of S_i and S_j may be between S_i and the reversed orientation of S_j. Reversing the orientation of a PRM spectrum S involves simply converting all of S's masses to SRMs by subtracting each PRM mass from the parent mass. Thus, S^R represents the reversed orientation of spectrum S with PRMs $\{p' = \text{PM}[S] - p, \forall\ p \in S\}$. The definitions in the table below are illustrated in Fig. 1*B*.

For each unique pair of contig PRM spectra (S_i,S_j), all possible shifts of S_j wrt S_i and S_j^R wrt S_i that yielded at least 6 matching peaks were considered and the shifts $A\langle S_i,S_j\rangle$ and $A\langle S_i,S_j^R\rangle$ were set. Of these two shifts, the shift with the highest score was reported for the pair. If score($A\langle S_i,S_j^R\rangle$) > score($A\langle S_i,S_j\rangle$), the reverse state of A, R[A], was set to *true* in order to indicate that S_j should be reversed wrt S_i (R[A] ← *false* otherwise). Given an input minimum score τ, alignments were then discarded if score(A) < τ. The parameter τ is also enforced in Meta-Assembly and was separately trained for low mass accuracy contig PRM spectra (0.5 Da peak tolerance) and high mass accuracy contig PRM spectra (0.05 Da peak tolerance).

Meta-Assembly—Similar to the SPS assembly of aligned PRM spectra into contigs, Meta-Assembly groups aligned contig PRM spectra into *meta-contigs*. Similar to the relationship between a contig and a contig PRM spectrum, every meta-contig also has a *meta-contig PRM spectrum*. Each meta-contig initially contains one contig PRM spectrum. As illustrated in Fig. 1*C*, Meta-assembly then iterates over the following steps: (1) *Recruit* → (2) *Reverse* → (3) *Re-sequence* → (4) *Re-score*. Step 1 finds the highest scoring aligned pair of meta-contigs $A^*\langle M_i,M_j\rangle$ and stops if the score is below threshold τ; Step 2 reverses M_j if required by the alignment; Step 3 merges M_i and M_j into M_i^* and determines the updated meta-contig PRM spectrum; Step 4 transfers and re-scores alignments from M_i and M_j to M_i^* and returns to Step 1.

The problem addressed by Meta-Assembly is in the context of an overlap graph (16), where each vertex is a meta-contig M_i initialized to SPS contig S_i and meta-contig vertices are connected by scored *alignment edges* labeled with shifts $A\langle M_i,M_j\rangle$, scores score($A\langle M_i,M_j\rangle$), and reverse states R[$A\langle M_i,M_j\rangle$] all initialized using alignments between the corresponding contigs, as described above. In a perfect graph, all connected meta-contigs can be aggregated by merging every alignment edge. However, even though contig PRM spectral alignments are much more reliable than alignments between PRM spectra derived directly from MS/MS spectra, there are still incorrect edges in the graph. There are two types of incorrect edges: *inconsistent* edges disagree on the shift of meta-contigs wrt each other and *incoherent* edges disagree on the orientation of meta-contigs wrt each other. For example, there may be three alignment edges $A_1\langle M_i,M_j\rangle$, $A_2\langle M_j,M_k\rangle$, and $A_3\langle M_i,M_k\rangle$ between three meta-contigs M_i, M_j, and M_k such that $A_1 + A_2 \neq A_3$. Here the path from M_i to M_k following A_1 and A_2 imposes a *transitive* shift (a shift imposed by two or more pair-wise alignments) between M_i and M_k that is not consistent with A_3. It may also be the case that R[A_3] = *true* while R[A_1] = R[A_2] = *false*. Here the edges are incoherent because A_1 and A_2 indicate that M_i, M_j, and M_k are in the same orientation whereas A_1 and A_3 indicate that M_k is reversed wrt M_i and M_j. The meta-contig assembly problem is that of finding and merging the maximal scoring subset of consistent and coherent alignment edges such that every contig PRM spectrum can be aligned to its meta-contig PRM spectrum with score at least τ. It has been shown that finding the maximal scoring subset of consistent and coherent edges is a hard problem (1). Thus, we propose an iterative algorithm to approach the optimal solution. See Supplemental Meta-Assembly for a detailed description of Meta-Assembly steps.

In step 1, we recruit the highest scoring edge $A^*\langle M_i,M_j\rangle$ between any two meta-contigs M_i and M_j. If score(A^*) < τ, then all remaining edges have a score below the threshold and the merging process ends. Otherwise, M_i and M_j are merged in steps 2–4.

In step 2, M_j is reversed if R[A^*] = *true*. As described in Spectral Alignment, some alignments between contig PRM spectra are in different orientations. Thus, if aligned contig PRM spectra are to be assembled into coherent meta-contigs, some of them will need to be reversed. In step 2, meta-contig M_j is reversed to M_j^R if R[A^*] = *true* to assure spectra inside M_i and inside M_j are in the same orientation before the meta-contigs are merged. The reversed meta-contig M_j^R is obtained from M_j by reversing all of its assembled contig PRM spectra and their relative alignments. Given an alignment shift $A\langle S_a,S_b\rangle$, its reversed alignment shift $A^R\langle S_a^R,S_b^R\rangle$ is equal to PM[S_a] − A − PM[S_b]. The final step in reversing M_j is to update the reverse state of alignment edges connected to it. For all alignment edges $A_k\langle M_j,M_k\rangle$ connecting M_j to other meta-contigs, A_k is also reversed and R[A_k] ← *not* R[A_k] to indicate whether M_k also needs to be reversed if it is to be merged to M_i and M_j in a subsequent iteration (only M_j is reversed in this iteration).

In step 3, M_i^* is created as the union of M_i and M_j and the meta-contig PRM spectrum of M_i^* is determined. A^* is used as the shift to connect contig PRM spectra in M_i to contig PRM spectra in M_j. So after $M_i^* \leftarrow (M_i \cup M_j)$, every contig PRM spectrum $S_x \in M_i$ is con-

$A\langle S_i,S_j\rangle$	Mass shift (in Da) of S_j *wrt* S_i *that yields the maximum score*(A)
MP(A)	Number of matched peak pairs between S_i and S_j
MI(A)$_i$	Summed intensity of all peaks in S_i that match peaks in S_j
MI(A)$_j$	Summed intensity of all peaks in S_j that match peaks in S_i
OI(A)$_i$	Summed intensity of all peaks in the *m/z* range of S_i *that overlaps with the aligned m/z* range of S_j
OI(A)$_j$	Summed intensity of all PRMs in the *m/z* range of S_j *that overlaps with the aligned m/z* range of S_i
score(A)	$\min\left(\frac{\text{MI}(A)_i}{\text{OI}(A)_i}, \frac{\text{MI}(A)_j}{\text{OI}(A)_j}\right)$*MP($A$)
R[A]	*true* if score($A\langle S_i,S_j^R\rangle$) > score($A\langle S_i,S_j\rangle$), *false* otherwise

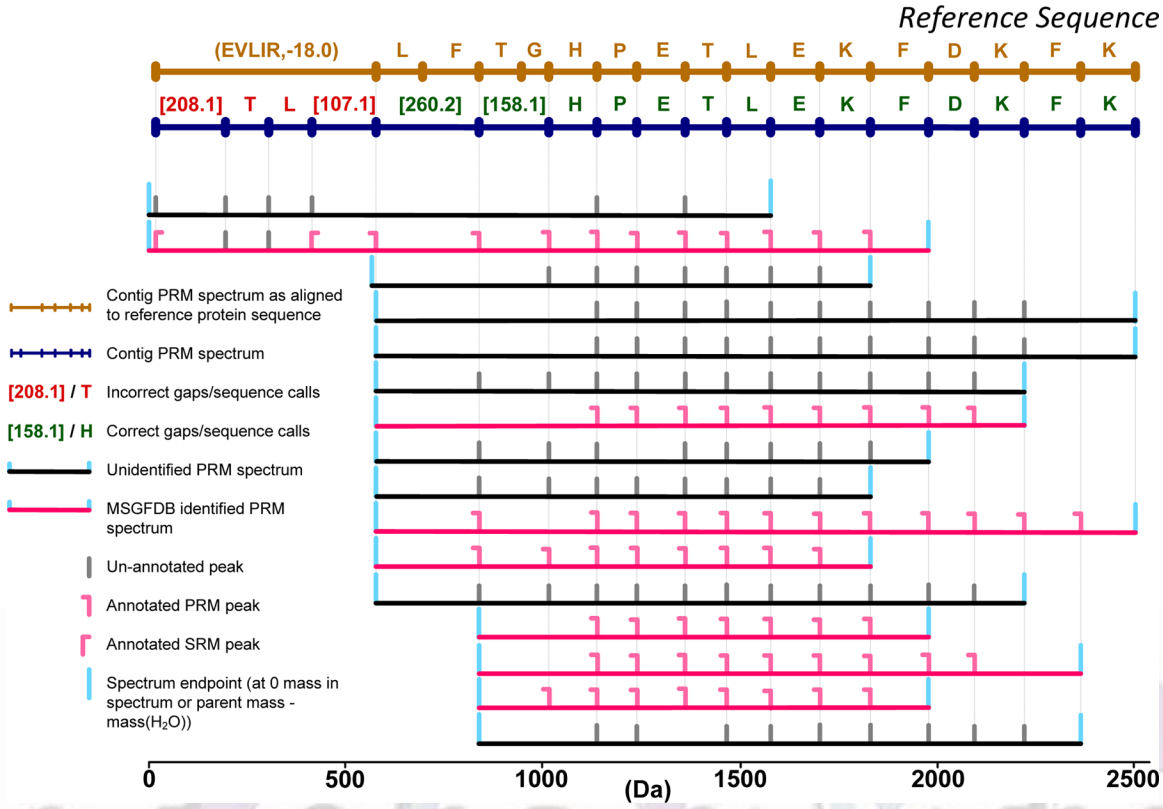

FIG. 2. **Annotation of contigs and meta-contigs with MS-GFDB spectrum identifications.** The annotation of a SPS contig is shown here but the same procedure applies for meta-contigs. Above the contig PRM spectrum are all sequence calls that align to the reference. Below the contig PRM spectrum are all spectra from overlapping peptides that were assembled to yield the contig PRM spectrum. Only assembled peaks are shown in each assembled PRM spectrum. For a sequence call to be labeled correct, it must be flanked by at least one pair of annotated PRM or SRM peaks in the same ion series that map to the same protein. If a sequence call that is not labeled correct is flanked by at least one pair of peaks from an identified spectrum then it is labeled incorrect. If a sequence call is not flanked by at least one pair of peaks from an identified spectrum then it is labeled un-annotated.

nected to every contig PRM spectrum $S_y \in M_j$ by the transitive shift $A\langle S_x,S_y\rangle = A\langle S_x,S_i\rangle + A^* + A\langle S_j,S_y\rangle$ where S_i and S_j were the first contig PRM spectra in M_i and M_j, respectively. Because only one shift is used to connect contig PRM spectra in M_i and M_j, all assembled alignments between spectra in M_i^* are guaranteed to be consistent because M_i and M_j are internally consistent. The contig PRM spectra and their spectral alignments in M_i^* are then used as input to SPS to determine its meta-contig PRM spectrum as in (1).

In step 4, alignment edges connected to M_i and M_j are re-scored and moved to M_i^*. For every M_k connected to M_i through some alignment edge $A_1\langle M_i,M_k\rangle$, $A_1^*\langle M_i^*,M_k\rangle \leftarrow A_1$ is used to connect M_i^* to M_k. If a M_k is connected to M_j through some alignment edge $A_2\langle M_j,M_k\rangle$, $A_2^*\langle M_i^*,M_k\rangle \leftarrow A^* + A_2$ is used to connect M_i^* to M_k. If a M_k is connected to both M_i and M_j through A_1 and A_2, A_1^* is used if score(A_1^*) > score(A_2^*) and A_2^* is used otherwise. After all edges are transferred from M_i and M_j to M_i^*, M_i and M_j are removed from the graph. Then the scores of all edges connected to M_i^* are updated for recruitment in step 1 of the next iteration.

Fig. 1*D* illustrates how this approach aggregates contigs connected by high scoring alignments before considering contigs with less reliable alignments. An important benefit of this property is that meta-contig sequences are reliably extended and updated (by merging high scoring alignment edges first) before they are used to re-score less reliable alignments. An alternative approach to further capitalize on this property by discovering new alignments between updated meta-contigs could be to add a step between *Re-score* and *Recruit* that re-aligns M_i^* to every other meta-contig in the overlap graph. This was attempted, but it significantly increased the running time of the implementation without yielding longer meta-contig sequences.

After iterative merging of meta-contigs, only meta-contigs that assemble at least 2 contig PRM spectra or more are reported. Also, contigs and meta-contigs were required to yield an amino acid subsequence of at least five consecutive residues.

RESULTS

The performance of Meta-SPS and SPS was assessed in reference to target protein sequences and compared with determine the effectiveness of these additions to the SPS workflow. Two separate procedures were used to evaluate the performance of SPS and Meta-SPS, which was mainly measured in terms of *de novo* sequencing length, coverage, and accuracy. First, PRM spectra identified by MS-GFDB at 1% spectrum-level FDR were used to annotate contig PRM spectra (described in Fig. 2) and determine *de novo* sequencing accuracy. If a contig assembled at least one identified PRM spectrum, the contig itself was labeled *identified*. Peptides IDs were then mapped to their corresponding protein IDs and used to annotate peaks in identified PRM spectra as

a) Sequencing accuracy as a function of position in meta-contig

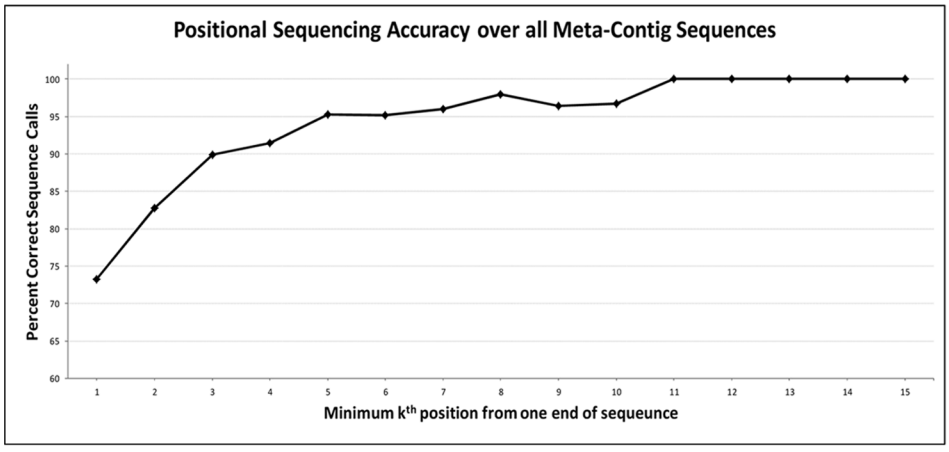

b) Meta-contig sequencing coverage, length, and accuracy

		6-Protein Mixture						aBLTA	
	Protein	P_1	P_2	P_3	P_4	P_5	P_6	P_7	P_8
	Protein Length (AA)	167	261	548	154	100	353	219	443
	Spectrum Coverage (%)	94.6	90.8	97.8	99.4	60.0	67.7	97.7	100
Coverage	Mapped Meta-contigs	6	8	20	9	5	13	7	20
Coverage	Sequencing Coverage (%)	70.1	78.5	80.7	83.1	52.0	42.2	87.7	90.7
Coverage	Coverage Redundancy	1.2	1.2	1.1	1.1	1.2	1.1	1.1	1.2
Coverage	Spectra Per Meta-contig	130	175	96	25	75	44	163	80
Coverage	Peptides Per Meta-contig	37	45	30	9	20	15	56	42
Coverage	Average Seq. Length (AA)	22.7	29.9	23.8	15.4	12.4	13.0	30.9	23.2
Coverage	Longest Sequence (AA)	45	91	47	25	17	21	106	60
Accuracy	Identified Meta-contigs	5	7	20	8	4	13	6	19
Accuracy	Correct Sequence Calls (%)	98.2	94.2	91.6	92.4	89.8	97.2	98.3	97.0
Accuracy	Un-annotated Seq. Calls (%)	1.8	2.6	4.3	0.8	5.8	1.4	3.3	9.6

FIG. 3. **De novo sequencing length, coverage, and accuracy.** *A*, The *x* axis plots the minimum distance (k) a sequence call or gap is from one end of a meta-contig sequence and the *y* axis plots the average sequencing accuracy over all annotated calls at each k-distance. Over all annotated calls reported more than 8 positions from their closest end, there were a total of 3 incorrect sequence calls at k = 20, 21, and 22 of a single meta-contig aligned to the aBTLA heavy chain (discussed in the Results section of Supplementary Materials). *B*, Protein identifiers are: P_1 - leptin precursor, P_2 - kallikrein-related peptidase, P_3 - GroEL, P_4 - myoglobin, P_5 - aprotinin, P_6 - peroxidase, P_7 - aBTLA light chain, and P_8 - aBTLA heavy chain. *Protein Length* is the length of each reference protein in amino acid residues. *Spectrum Coverage* is the percent of each protein covered by peptides identified MS-GFDB with 1% FDR. *Coverage* is taken over all mapped contigs and *Accuracy* is taken over all identified meta-contigs. Mapped meta-contigs must be aligned to a reference protein as described in the text whereas identified meta-contigs must assemble at least one identified spectrum whose peptide sequence is a substring of a reference protein. *Sequencing Coverage* is the percent of amino acids in each protein covered by at least one mapped meta-contig sequence. *Coverage Redundancy* is the average number of mapped meta-contig sequences covering each amino acid residue that is covered by at least one meta-contig sequence. *Spectra Per Meta-contig* is the average number of spectra assembled by each mapped meta-contig whereas *Peptides Per Meta-contig* is the average number of peptides (spectra with distinct parent masses) assembled by each mapped meta-contig. *Average Seq. Length* is the average number of amino acid residues covered by each mapped meta-contig and *Longest Sequence* is the maximum number of amino acid residues covered by a mapped meta-contig. *Correct Sequence Calls* is the percentage of annotated sequence calls that were correct in identified meta-contigs. *Un-annotated Seq. Calls* is the percentage of sequence calls that were un-annotated in identified meta-contigs.

PRMs or SRMs. Mass differences between consecutive peaks in contig PRM spectra (*i.e.* sequence calls or gaps) were labeled using peaks from the annotated PRM spectra they assembled (Fig. 2). A contig sequence call was labeled *annotated* if its flanking peaks each assemble a mass from the same identified PRM spectrum. An annotated sequence call was *correct* if its flanking peaks assemble spectrum masses in the same ion series in the same identified spectrum (*i.e.* both are identified PRMs or both are identified SRMs) on the same protein. Annotated sequence calls not labeled correct are labeled *incorrect*. Because meta-contigs assemble contigs, every peak in a meta-contig PRM spectrum also assembles a set of PRM masses. Therefore, meta-contigs are annotated in the same manner as contigs.

The graph displayed in Fig. 3*A* demonstrates that sequencing errors are localized toward the ends of sequences and are F3

not distributed randomly. This occurs because often more PRM spectra overlap toward the middle of contig and meta-contig sequences, which gives a stronger consensus sequence. Given that sequence calls at the first or last residue of every meta-contig sequence were 20% less accurate than sequence calls two or more positions in from both ends, we truncated every meta-contig and contig sequence by one sequence call from each end. This post-processing step had the effect of increasing sequencing accuracy by roughly 2% over all contig and meta-contig sequences at a limited loss in sequencing coverage. Meta-contigs were then 94% accurate (1 error per 18 AA) over all 6-prot proteins and 97% (1 error per 35 AA) accurate over the aBTLA antibody (Fig. 3*B*) whereas SPS contigs were 88% accurate (1 error per 8 AA) over all 6-prot proteins and 96% accurate (1 error per 25 AA) over the aBTLA antibody (supplemental Table S3). ZSI

MS-GFDB IDs could also have been used to evaluate sequencing coverage and length, but because less than 45% of spectra assembled into contigs and meta-contigs were identified in both data sets, such an approach would ignore many contigs that assemble unidentified spectra. Thus, contig and meta-contig PRM spectra were also directly mapped to reference proteins to evaluate *de novo* sequencing coverage and length. Contig spectra were aligned to protein sequences using an algorithm similar to MS-Alignment (37, 38). The protein sequences were first converted to perfect, unmodified PRM spectra and they were aligned (as in supplemental Fig. S1) to contig and meta-contig PRM spectra requiring at least seven matching peaks. ZSI Alignments of contig PRM spectra were allowed with one modification to capture PTMs and meta-contig PRM spectra were allowed with at most two modifications because of their increased length. A contig or meta-contig that was aligned to a reference protein in this manner is termed *mapped*. Roughly 50% more SPS contigs were mapped than were identified over both data sets, which is expected as many contigs assemble low-quality MS/MS spectra that are often left unidentified at 1% FDR. Only about 10% more meta-contigs were mapped than were identified, which is also expected as ~5X more spectra were assembled per meta-contig than for SPS contigs. To evaluate the accuracy of the alignment mappings, the mapped residue locations of aligned contig and meta-contig PRM peaks were compared with those of assembled annotated peaks in MS-GFDB identified spectra. Over all aligned contig and meta-contig PRM peaks that assembled at least one mass from an identified spectrum, greater than 95% were aligned to the same residue as at least one their assembled masses. 593 of 666 (89%) 6-prot SPS contigs were mapped to target or contaminant proteins (482 mapped to target proteins) whereas for 6-prot, all 68 meta-contigs were mapped (64 mapped to target proteins). Similarly, 290 of 329 (88%) aBTLA SPS contigs were mapped (192 mapped to the antibody sequence) whereas all 43 aBTLA meta-contigs were mapped (27 mapped to the antibody sequence).

Figs. 3*A* and 3*B* illustrate the resulting meta-contig coverage for kallikrein-related peptidase and aBTLA light chain, respectively. Supplemental Figs. S5–S10 materials illustrate meta-contig coverage for remaining 6-prot proteins as well as the aBTLA heavy-chain. The largest meta-contig in Fig. 4*A* (colored red) corresponds to a 91 AA meta-contig sequence covering more than one third of the protein. The yellow meta-contig in Fig. 4*A* appears to have sufficient overlap with neighboring blue and purple meta-contigs to combine them, but the ends of the three meta-contig sequences contained too many gaps (seven missing PRMs) and incorrect sequence calls (two incorrect PRMs) to exceed the current acceptance threshold of sharing six or more matching peaks (supplemental Fig. S3). Such gaps and errors stem from incomplete MS/MS peptide fragmentation. In the discussion section we describe foreseeable data acquisition and algorithmic adjustments that could either generate data with higher sequence content and/or enable reducing the acceptance threshold without diminishing sequencing accuracy. In Fig. 4*B*, the largest meta-contig (colored orange) corresponds to a 106 AA meta-contig sequence covering more than one half of the target protein. See Fig. 3*B* for meta-contig coverage statistics on all proteins and see supplemental Materials for SPS contig coverage statistics in the same format. *De novo* sequencing gave 83% of MS-GFDB coverage between both data sets and we observe much higher sequence coverage of the purified aBTLA antibody (89%) compared with 6-prot proteins (42–83%). Because the heavy and light chains of the aBTLA antibody were purified prior to MS/MS analysis, higher aBTLA sequencing coverage is expected as more spectra from distinct peptides were identified by MS-GFDB per target protein in the aBTLA sample compared with the 6-prot sample (Fig. 3*A*). This is not an algorithmic limitation of our approach, but rather limitations of subcellular protein processing and MS/MS data acquisition. The lack of coverage of certain regions of the kallikrein-related peptidase in Fig. 4*A* is expected. The commercially obtained protein used in these studies was purified from human seminal fluid. Thus, it can be expected to lack the N-terminal region 1–24 because of prior cleavage of the signal peptide, residues 1–17, and activation by cleavage of the propeptide, residues 17–24. Furthermore, *N*-linked glycosylation is known to occur at residue 69. The subsequent sugar micro-heterogeneity at that position should render any individual proteolytically-generated peptide containing that residue much less concentrated in the digestion mixture, and if subjected to MS/MS much less likely to yield interpretable fragmentation. ZSI F4 ZSI ZSI

SPS contig alignments were also used to train the minimum spectrum alignment score τ to impose in *Spectral Alignment* and *Meta-Assembly*. τ was trained such that at least 97% of transitive alignments (alignments induced by two or *more* pair-wise alignments) between mapped contig PRM spectra in the same meta-contig were correct (a correct alignment is one whose observed shift matches the theoretical shift within

a) Meta-contig coverage of kallikrein-related peptidase

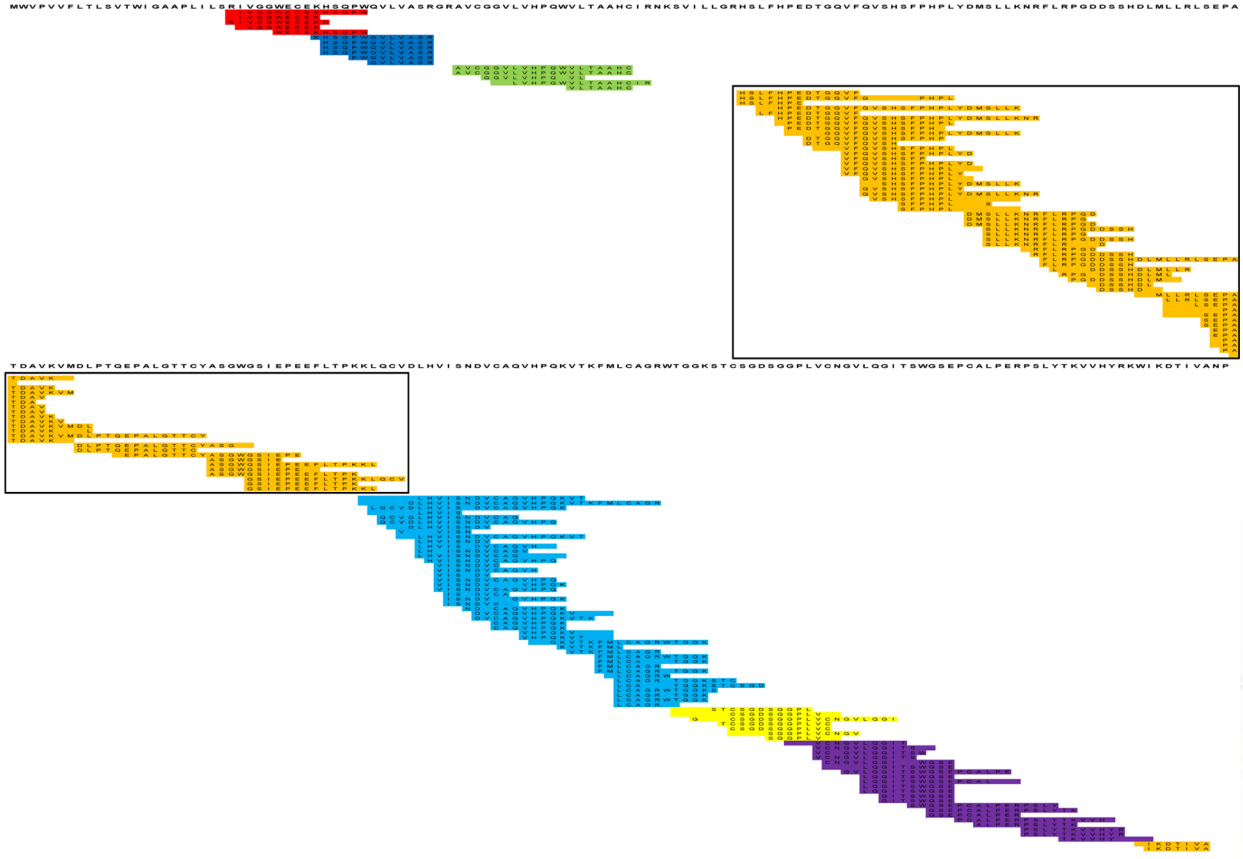

[SL]FH[PE]D[TG]QVFQV[SH][SF][PH]PLY[DM]SLLKNR[FL]R[PG]DDSSHDLMLLRLSE[PA]ELTDAVKVMDL[PT]QE[PA]LG[TT]CY[AS]GWGSIE[PE]EFLT[PK]

b) Meta-contig coverage of aBTLA light chain

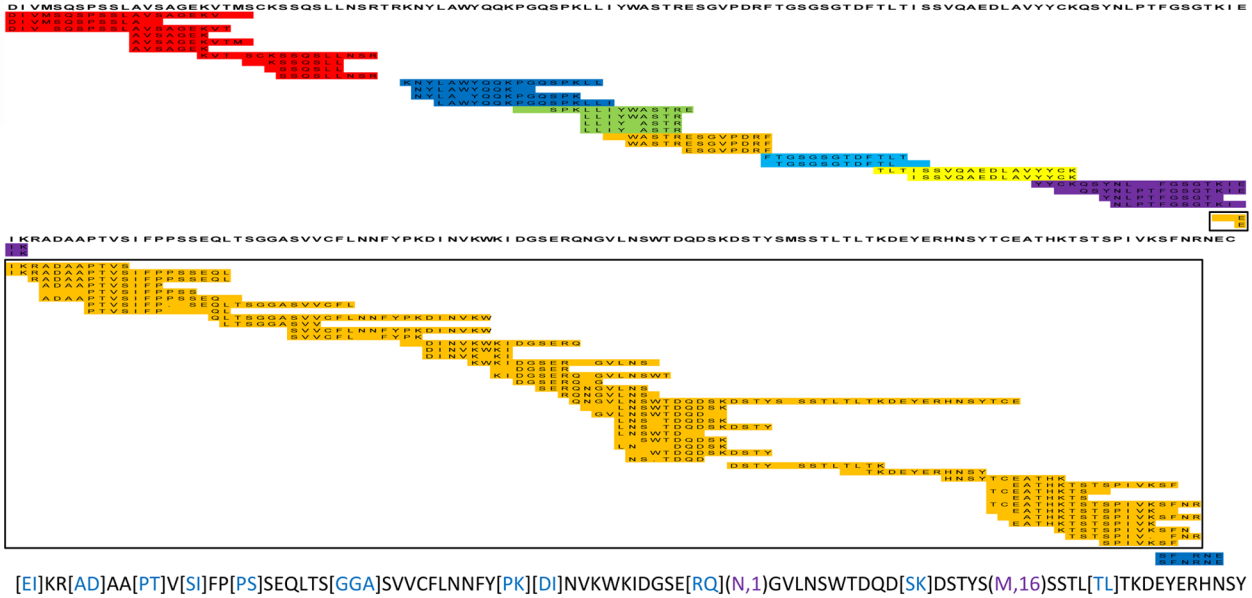

[EI]KR[AD]AA[PT]V[SI]FP[PS]SEQLTS[GGA]SVVCFLNNFY[PK][DI]NVKWKIDGSE[RQ](N,1)GVLNSWTDQD[SK]DSTYS(M,16)SSTL[TL]TKDEYERHNSY TCEATHK[TS]TS[PI]VK[SF]N

the mass of a PTM). Over both data sets, 91% of all correct alignments were retained between pairs of mapped contig PRM spectra with at least 6 matching peaks. τ was trained to be 2.8 for 6-prot data, 3.0 for aBTLA, and can be estimated for any data set using a subset of identified spectra. After alignments with scores less than τ were removed (just prior to Meta-Assembly), 99% of all pair-wise alignments between mapped contig PRM spectra with at least 6 matching peaks were reported at 90% accuracy. But if transitive alignments were also considered, only 23% of alignments were correct because of the incorrect alignments reported by *Spectral Alignment*, those between components of multiple aligned contigs induced many more incorrect transitive alignments. The iterative merging procedure of Meta-Assembly was effective at discarding such incorrect alignments as 97% of transitive alignments ultimately reported were correct (supplemental Fig. S4).

The efficiency of Meta-SPS merging of SPS contigs is indicated by the decrease in coverage redundancy from 3.7 (supplemental Table S3) to 1.1 (Fig. 3*A*) as contigs covering the same regions were aggregated into meta-contigs. But because meta-contigs must assemble at least two contigs, meta-contigs do not cover regions missed by SPS contigs (*i.e.* coverage can only decrease from contigs to meta-contigs). Meta-contigs covered roughly 10% less of the 6-prot proteins than SPS contigs and 2% less of the aBTLA antibody. Thus, we generally observed a drop in coverage as a trade-off for Meta-SPS's higher sequencing accuracy. Coverage can be recovered by using "leftover" SPS contigs that were not merged by Meta-SPS, although lower sequencing accuracy is to be expected for certain applications (supplemental Table S2).

Meta-SPS also had the effect of doubling the average length of SPS contig sequences (to 20 AA in 6-prot meta-contigs and 25 AA in aBTLA meta-contigs) and tripling their maximum length (to 91 AA over 6-prot meta-contigs and 106 AA over aBTLA meta-contigs). Furthermore, the longest meta-contigs yielded the highest sequencing accuracy as the 91 AA and 106 AA *de novo* sequences displayed in Figs. 3*A* and 3*B*, respectively, were 100% annotated and correct. Although one peak in the 91 AA sequence incorrectly assembled masses mapping to different residues, this error was not reflected in the final sequence because the majority of the peak's assembled masses mapped to the correct residue.

The running time of Spectral Alignment and Meta-Assembly was found to be minor ($<$ 9 min for the 6-prot data set) in comparison to that of SPS, which requires an all-to-all alignment of PRM spectra (see supplemental Materials for a more detailed description). All SPS contigs, meta-contigs, input MS/MS spectra, identified spectra, and annotated *de novo* sequences associated with this paper may be downloaded from Tranche/ProteomeCommons.org at the following hash:

s+8iy5TbHHydsOPmTf9yqotRGvkxeJPF8BXJxMxxZOnCRXqbje8wbn+Orpxr51YR3L0S2sZBTYljUdHUF35LjfTqeukAAAAAAv6xWQ==. This link also contains *de novo* sequencing reports that visualize how MS/MS spectra from each data set were used to generate *de novo* protein sequences. A subset of these reports detailing all 6-prot meta-contigs can also be found directly at http://proteomics.ucsd.edu/Software/MetaSPS/6-prot_meta-contigs/index.html. in supplemental Fig. S11 materials provides a description of how to interpret these reports in relation to algorithmic steps outlined Fig. 1*A*.

Although the 6-prot sample contained a mixture of proteins, applications of *de novo* protein sequencing are often targeted toward specific proteins within a larger mixture. To test how Meta-SPS performance might be impacted by such samples, we combined the 6-prot CID MS/MS spectra with the high resolution CID MS/MS spectra from the aBTLA sample and executed the algorithmic steps outlined in Fig. 1*A* on the combined set of MS/MS spectra. Here, the proteins of interest were the heavy and light chain of aBTLA antibody and the background mixture was represented by the 6-prot data. Because the high resolution CID spectra from the aBTLA and 6prot samples were acquired on a similar model of instrument (LTQ Orbitrap XL and LTQ Orbitrap, respectively), the low-resolution aBTLA spectra were excluded from this experiment to better simulate high resolution data acquisition of an aBTLA/6-prot mixture sample. Although this does not rigorously simulate the expected loss in MS/MS coverage one might expect from such a mixture (because of incomplete peptide sampling by the instrument), it is still a fair approximation of the algorithmic challenges associated with sequencing a small subset of proteins within the background of higher complexity. In practice, one would simply extend the LC gradient time or collect the data on a faster scanning instrument in order to maintain adequate peptide sampling. Compared with sequencing results on the aBTLA high reso-

FIG. 4. **Mapped Meta-contigs.** Meta-contig PRM spectra were aligned to reference proteins to evaluate *de novo* sequencing coverage. Every colored row corresponds to a contig PRM spectrum as separately mapped to the target protein sequence (information not used by Meta-SPS). Every set of overlapping contigs of the same color corresponds to a meta-contig; sets of contigs of the same color with no overlap indicate separate meta-contigs. Below each coverage map is the longest meta-contig sequence of the boxed meta-contig for the corresponding protein. *Purple* gaps correspond to mapped sequence calls with PTMs verified by MS-GFDB; blue gaps correspond to mapped gaps that span 2 or more residues in the reference. Remaining un-colored residues represent sequence calls that map to reference amino acid masses. *A*, Meta-contig coverage of kallikrein-related peptidase from the 6-prot sample is displayed here; 8 meta-contigs covered 78% of the 261 AA protein with the longest sequence spanning 94 AA. *B*, Meta-contig coverage of the aBTLA light chain is displayed here; 9 meta-contigs covered 87% of the 219 AA protein with the longest sequence spanning 107 AA.

lution spectra, Meta-SPS produced the same sequencing accuracy (98.1% compared with 98.6%) and average length (18 AA compared with 17 AA) of the aBTLA antibody from the combined aBTLA/6-prot set of MS/MS spectra at the cost of reduced sequencing coverage (58% compared with 71%) and shorter maximum sequence length (35 AA compared with 45 AA). Compared with SPS, Meta-SPS generated *de novo* sequences 100% longer on average from the combined set with ~2x as many correct sequence calls per incorrect sequence call. We note that in a real MS experiment mixing the 6-prot and aBTLA samples, the absence of a faster spectral acquisition rate and/or extended peptide separation time could diminish protein sequence coverage by MS/MS spectra and thus further limit the overall sequencing length and coverage.

DISCUSSION

Shotgun protein sequencing with meta-contig assembly is a modification-tolerant method for de novo protein sequence reconstruction. We demonstrate that extensive and accurate protein sequencing can be achieved without the use of a database, meaning more can be gained from experimental MS/MS data before mapping to a reference database. Compared with any other automated approach, our method provides the longest and most accurate de novo sequences without requiring any sequence homology steps. Furthermore, we demonstrate that de novo sequences which extend beyond 90 amino acids can be assembled with 100% accuracy. In the shorter sequences we report sequencing errors that are not distributed randomly, but located overwhelmingly toward the ends of sequences (Fig.3 *A*).

Meta-SPS offers an effective improvement to Shotgun Protein Sequencing by doubling the average length of SPS de novo sequences, tripling their maximum sequence length, reducing sequence coverage redundancy ~4X, and increasing sequencing accuracy 4–5%. There was only one protein, myoglobin, whose meta-contig sequences were less accurate (by 3%) than its SPS contig sequences (supplementary Table S3). In this case there were no sequencing errors introduced in myoglobin's meta-contig sequences that were not already present in its SPS contig sequences. But rather there was little overlap between incorrect and correct SPS sequence calls. When incorrect SPS contig sequence calls overlap with multiple correct contig sequences at multiple positions in the protein sequence, Meta-SPS can repair the incorrect sequence calls in meta-contigs at those positions if the correct calls are the consensus. But if such overlaps occur with limited frequency, as in the case of myoglobin, the reduced percentage of correct sequence calls (because of SPS contig redundancy) is greater than the reduced percentage of incorrect sequence calls in meta-contig sequences. This has the effect of lowering the observed percentage of correct calls from contig to meta-contig sequences.

Although Meta-SPS fell short of fully reconstructing a protein sequence in either data set, it assembled *de novo* sequences up to 91 AA long for a protein mixture and 106 AA long for a purified antibody, which are the longest confirmed *de novo* sequences ever obtained from the automated analysis of unidentified MS/MS spectra. Furthermore, 11 sequences from 6-prot and 6 sequences from aBTLA were extended beyond 40 AA. Sequencing accuracy was 95% for aBTLA and 6-prot samples, whereas the 91 AA and 106 AA sequences were 100% accurate. If we remove the first and last two residues or gaps of every sequence (where there was weaker consensus on average), sequencing accuracy improves to 96% over 6-prot proteins and 98% over the aBTLA antibody. Increased accuracy and reduced coverage redundancy of meta-contigs compared with SPS contigs was achieved at the cost of reduced meta-contig coverage (10% less coverage of 6-prot proteins and 2.5% less coverage of the aBTLA antibody).

Full reconstruction of protein sequence encoded by the genome is subject to limitations of sub cellular protein processing and posttranslational modification. When a protein is purified from its biological source it can be expected to have N and C-terminal signal peptides and pre-pro activation sequences already cleaved off (39). Although these can be predicted from a gene sequence, when a protein isolated from an organism with an un-sequenced genome is sequenced by the process described here, one would not be certain of having obtained the protein termini, unless they were chemically labeled prior to digestion (40). Furthermore, in higher organisms *N*-linked glycosylation can occur at NX(S/T) motifs, particularly for secreted and extracellular membrane proteins (41). Unless, the protein is de-glycosylated with an enzyme like PNGase-F, prior to proteolytic digestion, the sugar microheterogeneity at those sites should render any individual proteolytically-generated peptides containing the Asn residue from the motif much less concentrated in the digestion mixture, and if subjected to MS/MS much less likely to yield interpretable fragmentation.

As with SPS sequencing, Meta-SPS also faces limitations related to proteomics mass spectrometry, such as incomplete enzyme digestion, peptide sampling bias, and ambiguous amino acid masses (17). Cleaved peptides are not equally sampled by MS/MS instrumentation (e.g. hydrophobicity, ionizability, location of basic residues, etc.), leading to biased peptide coverage of target proteins. Furthermore, certain combinations of amino acids have identical masses and may lead to ambiguity in the final sequences (Ile = Leu = 113, GG = Asn = 114, and GA = Gln = 128). Because we require large sets of MS/MS spectra from overlapping peptides covering an entire protein to generate long sequences, we also face limitations when analyzing complex mixtures of proteins and proteins with related sequences. Our method is currently optimized for small mixtures of unrelated proteins or purified proteins, as we observe that coverage and sequence length degrade as fewer quality spectra are acquired per protein in the sample (Fig. 3*B*). Nonetheless, even in the background of

ZSI

the 6prot MS/MS spectra, Meta-SPS still improved upon SPS sequencing accuracy (from 97% to 98%), average sequence length (from 11 AA to 20 AA), and maximum sequence length (from 25 AA to 35 AA) for the aBTLA antibody. Analyzing more complex mixtures with greater effectiveness may require faster spectral acquisition rates or extended peptide separations to generate enough spectra to cover all proteins in a sample.

To enable assembling longer meta-contigs and achieve higher protein coverage a few adjustments to both data acquisition and algorithmic strategies are currently foreseeable. Compared with the use of CID and/or HCD fragmentation, it has been shown that electron transfer dissociation (ETD) can yield more interpretable MS/MS spectra from more unique peptides and greatly increase the number of interpretable spectra from longer peptides (with precursor charge 3^+ or higher) (42, 43). The high resolution CID and HCD spectra described were collected in separate LC-MS/MS runs on a first generation LTQ Orbitrap that is not equipped with ETD. However, the duty cycle on newer LTQ Velos Orbitrap instruments is more than twice as fast. Thus in nearly equivalent chromatographic run time the newer instruments can subject each precursor ion to CID, HCD, and ETD fragmentation in 3 consecutive high resolution MS/MS spectra to provide information that is not only overlapping and complementary, but also all 3 can be directly attributed to the same peptide sequence. To support the combined processing of ETD, CID, and HCD spectra, spectral alignment steps in SPS will have to support alignments between b/c and y/z-type ions all the way from detection of pairs of spectra from overlapping peptides, through assembly of pairwise alignments into multiple alignments, and finally during the consensus interpretation of assembled ABruijn contigs.

Furthermore, high resolution MS/MS spectra allow for more accurate determination of true amino acid mass differences between MS/MS peaks and helps distinguish those from incorrect amino acid predictions in de novo sequencing applications (15). Although most results described here were achieved with high resolution MS/MS spectra acquired with ±15 ppm fragment mass accuracy, a fixed 0.05 Da fragment tolerance was imposed as SPS was not originally designed to support ppm tolerance. The 15 ppm is equivalent to 0.0015 Da at mass 100 and 0.06 Da at mass 4000. Implementing ppm tolerance in the Meta-SPS pipeline will impose much tighter tolerances in the mid-low mass range (0~2000 Da) and allow alignments of N- and C- terminal fragment peaks in MS/MS spectra from overlapping peptides to be more reliably separated from random alignments of noise peaks. This should also improve the separation of correct and incorrect contig/contig alignments in the Meta-Assembly step. In *particular, Meta-SPS currently requires* six or more matching peaks to confidently align PRM spectra of overlapping peptides but implementation of ppm tolerance could enable decreasing this threshold without diminishing sequencing accuracy.

The six matching peak requirement further translates into a five consecutive amino acid minimum overlap requirement in pair-wise peptide alignments. However, the proteolytic enzymes currently in common usage have overlapping specificities. For example trypsin cleaves at the C-terminal side of Lys and Arg, whereas Lys-C cleaves only at Lys and Arg-C cleaves only at Arg. Thus in a combined data set peptide triplets often result where two shorter peptides are present that when concatenated are the equivalent of a longer peptide that is also present, but our current algorithmic approach makes only pairwise comparisons. Thus we expect to better capitalize on the enzyme specificity by introducing a step that attempts to concatenate the PRM spectra of 2 smaller peptides prior to comparison to the PRM spectrum of a larger peptide when the sum of the 2 precursor masses matches the larger one after adjusting for precursor charge and the mass difference because of terminal groups added upon peptide bond cleavage. Consequently, we foresee these data acquisition and algorithmic strategy improvements will most likely yield longer, more accurate meta-contig sequences and higher protein coverage.

* This work was partially supported by the National Institutes of Health Grant 1-P41-RR024851 from the National Center for Research Resources. This work was also supported in part by a grant to Steven A. Carr from the NCI, National Institutes of Health (1U24 CA126476-02), part of NCI's Clinical Proteomic Technologies Initiative.

ZSI

[S] This article contains supplemental Tables S1 to S4 and Figs. S1 to S10.

AQ: B

‖ To whom correspondence should be addressed: Department of Computer Science and Engineering, University of California at San Diego, 9500 Gilman Dr., La Jolla, CA 92093. E-mail: aguthals@cs.ucsd.edu.

REFERENCES

1. Bandeira, N., Clauser, K. R., and Pevzner, P. A. (2007) Shotgun protein sequencing: assembly of peptide tandem mass spectra from mixtures of modified proteins. *Mol. Cell. Proteomics* **6,** 1123–1134
2. Bandeira, N., Pham, V., Pevzner, P., Arnott, D., and Lill, J. R. (2008) Automated de novo protein sequencing of monoclonal antibodies. *Nat. Biotechnol.* **26,** 1336–1338
3. Yates, J. R., 3rd, Eng, J. K., McCormack, A. L., and Schieltz, D. (1995) Method to correlate tandem mass spectra of modified peptides to amino acid sequences in the protein database. *Anal. Chem.* **67,** 1426–1436
4. Perkins, D. N., Pappin, D. J., Creasy, D. M., and Cottrell, J. S. (1999) Probability-based protein identification by searching sequence databases using mass spectrometry data. *Electrophoresis* **20,** 3551–3567
5. Tanner, S., Shu, H., Frank, A., Wang, L. C., Zandi, E., Mumby, M., Pevzner, P. A., and Bafna, V. (2005) InsPecT: Identification of Posttranslationally Modified Peptides from Tandem Mass Spectra. *Anal. Chem.* **77,** 4626–4639
6. Di Noia, J. M., and Neuberger, M. S. (2007) Molecular mechanisms of antibody somatic hypermutation. *Ann. Rev. Biochem.* **76,** 1–22
7. Maggon, K. (2007) Monoclonal antibody "gold rush". *Curr. Med. Chem.* **14,** 1978–1987
8. Haurum, J. S. (2006) Recombinant polyclonal antibodies: the next generation of antibody therapeutics? *Drug Discovery Today* **11,** 655–660
9. Duncan, M. W., Aebersold, R., Caprioli, R. M. (2010) The pros and cons of peptide-centric proteomics. *Nat. Biotechnol.* **28,** 659–664
10. Thoma, R. S., Smith, J. S., Sandoval, W., Leone, J. W., Hunziker, P.,

Hampton, B., Linse, K. D., and Denslow, N. D. (2009) The ABRF Edman Sequencing Research Group 2008 Study: investigation into homopolymeric amino acid N-terminal sequence tags and their effects on automated Edman degradation. *J. Biomol. Tech.* **20,** 216–225

11. Xiang, B., Walters, J., Mawuenyega, K., Simpson, J., Sandoval, W., Smith, J. S., and Hunziker, P. (2010) Results of the PSRG 2010 Study: Edman and Mass Spectrometric Terminal Sequencing of a Monoclonal Antibody, **21,** S18
12. Johnson, R. S., and Biemann, K. (1987) The primary structure of thioredoxin from Chromatium vinosum determined by high-performance tandem mass spectrometry. *Biochemistry* **26,** 1209–1214
13. Frank, A., and Pevzner, P. A. (2005) PepNovo: de novo peptide sequencing via probabilistic network modeling. *Anal. Chem.* **77,** 964–973
14. Ma, B., Zhang, K., Hendrie, C., Liang, C., Li, M., Doherty-Kirby, A., and Lajoie, G. (2003) PEAKS: powerful software for peptide de novo sequencing by tandem mass spectrometry. *Rapid Commun. Mass Spectrom.* **17,** 2337–2342
15. Chi, H., Sun, R. X., Yang, B., Song, C. Q., Wang, L. H., Liu, C., Fu, Y., Yuan, Z. F., Wang, H. P., He, S. M., Dong, M. Q. (2010) pNovo: de novo peptide sequencing and identification using HCD spectra. *J. Proteome Res.* **9,** 2713–2724
16. Bandeira, N., Tang, H., Bafna, V., and Pevzner, P. (2004) Shotgun protein sequencing by tandem mass spectra assembly. *Anal. Chemi.* **76,** 7221–7233
17. Mann, M., and Wilm, M. (1994) Error-tolerant identification of peptides in sequence databases by peptide sequence tags. *Anal. Chem* **66,** 4390–4399
18. Frank, A., Tanner, S., Bafna, V., and Pevzner, P. (2005) Peptide Sequence Tags for Fast Database Search in Mass-Spectrometry ~~research articles~~. *J. Proteome Res.*, 1287–1295
19. Huang, L., Jacob, R. J., Pegg, S. C., Baldwin, M. A., Wang, C. C., Burlingame, A. L., and Babbitt, P. C. (2001) Functional assignment of the 20 S proteasome from Trypanosoma brucei using mass spectrometry and new bioinformatics approaches. *J. Biol. Chem.* **276,** 28327–28339
20. Kim, S., Na, S., Sim, J. W., Park, H., Jeong, J., Kim, H., Seo, Y., Seo, J., Lee, K. J., and Paek, E. (2006) MODi: a powerful and convenient web server for identifying multiple post-translational peptide modifications from tandem mass spectra. *Nucleic Acids Res.* **34,** W258–63
21. Dasari, S., Chambers, M. C., Slebos, R. J., Zimmerman, L. J., Ham, A. J., and Tabb, D. L. (2010) TagRecon: high-throughput mutation identification through sequence tagging. *J. Proteome Res.* **9,** 1716–1726
22. Shilov, I. V., Seymour, S. L., Patel, A. A., Loboda, A., Tang, W. H., Keating, S. P., Hunter, C. L., Nuwaysir, L. M., and Schaeffer, D. A. (2007) The Paragon Algorithm, a next generation search engine that uses sequence temperature values and feature probabilities to identify peptides from tandem mass spectra. *Mol. Cell. Proteomics* **6,** 1638–1655
23. Taylor, J. A., and Johnson, R. S. (1997) Sequence database searches via de novo peptide sequencing by tandem mass spectrometry. *Rapid Commun. Mass Spectrom.* **11,** 1067–1075
24. Shevchenko, A., Sunyaev, S., Loboda, A., Bork, P., Ens, W., and Standing, K. G. (2001) Charting the proteomes of organisms with unsequenced genomes by MALDI-quadrupole time-of-flight mass spectrometry and BLAST homology searching. *Anal. Chem.* **73,** 1917–1926
25. Mackey, A. J. (2001) Getting More from Less: Algorithms for Rapid Protein Identification with Multiple Short Peptide Sequences. *Mol. Cell. Proteomics* **1,** 139–147
26. Han, Y., Ma, B., and Zhang, K. (2004) SPIDER: software for protein identification from sequence tags with de novo sequencing error. ~~*Proc. IEEE Computational Sys. Bioinformatics Conference* 206–15~~
27. Searle, B. C., Dasari, S., Wilmarth, P. A, Turner, M., Reddy, A. P., David, L. L., Nagalla, S. R. (2005) Identification of protein modifications using MS/MS de novo sequencing and the OpenSea alignment algorithm. *J. Proteome Res.* **4,** 546–554
28. Shen, Y., Tolić, N., Hixson, K. K., Purvine, S. O., Anderson, G. A., and Smith, R. D. (2008) De novo sequencing of unique sequence tags for discovery of post-translational modifications of proteins. *Anal. Chem.* **80,** 7742–7754
29. Bandeira, N., Tsur, D., Frank, A., and Pevzner, P. A. (2007) Protein identification by spectral networks analysis. *Proc. Natl. Acad. Sci. U. S. A.* **104,** 6140–6145
30. Liu, X., Han, Y., Yuen, D., and Ma, B. (2009) Automated protein (re)sequencing with MS/MS and a homologous database yields almost full coverage and accuracy. *Bioinformatics* **25,** 2174–2180
31. Castellana, N. E., Pham, V., Arnott, D., Lill, J. R., and Bafna, V. (2010) Template proteogenomics: sequencing whole proteins using an imperfect database. *Mol. Cell. Proteomics* **9,** 1260–1270
32. Castellana, N. E., Payne, S. H., Shen, Z., Stanke, M., Bafna, V., and Briggs, S. P. (2008) Discovery and revision of Arabidopsis genes by proteogenomics. *Proc. Natl. Acad. Sci. U. S. A.* **105,** 21034–21038
33. Kim, S., Mischerikow, N., Bandeira, N., Navarro, J. D., Wich, L., Mohammed, S., Heck, A. J., and Pevzner, P. A. (2010) The generating function of CID, ETD, and CID/ETD pairs of tandem mass spectra: applications to database search. *Mol. Cell. Proteomics* **9,** 2840–2852
34. Frank, A. M., Bandeira, N., Shen, Z., Tanner, S., Briggs, S. P., Smith, R. D., and Pevzner, P. A. (2008) Clustering millions of tandem mass spectra. *J. Proteome Res.* **7,** 113–122
35. Frank, A. M., Savitski, M. M., Nielsen, M. L., Zubarev, R. A., and Pevzner, P. A. (2007) De novo peptide sequencing and identification with precision mass spectrometry. *J. Proteome Res.* **6,** 114–123
36. Dancík, V., Addona, T. A., Clauser, K. R., Vath, J. E., and Pevzner, P. A. (1999) De novo peptide sequencing via tandem mass spectrometry. *J. Computational Biol.* **6,** 327–342
37. Pevzner, P. A., Dancíkm V., Tang, C. L. (2000) Mutation-tolerant protein identification by mass spectrometry. *J. Computational Biol.* **7,** 777–787
38. Tsur, D., Tanner, S., Zandi, E., Bafna, V., and Pevzner, P. A. (2005) Identification of post-translational modifications by blind search of mass spectra. *Nat. Biotechnol.* **23,** 1562–1567
39. Leversen, N. A., DeSouza, G. A., Målen, H., Prasad, S., Jonassen, I., and Wiker, H. G. (2009) Evaluation of signal peptide prediction algorithms for identification of mycobacterial signal peptides using sequence data from proteomic methods. *Microbiology* **155,** 2375–2383
40. Takahashi, T., Muneoka, Y., Lohmann, J., Lopez, de Haro, M. S., Solleder, G., Bosch, T. C., David, C. N., Bode, H. R., Koizumi, O., Shimizu, H., Hatta, M., Fujisawa, T., and Sugiyama, T. (1997) Systematic isolation of peptide signal molecules regulating development in hydra: LWamide and PW families. *Proc. Natl. Acad. Sci. U. S. A.* **94,** 1241–1246
41. Larkin, A., and Imperiali, B. (2011) The expanding horizons of asparagine-linked glycosylation. *Biochemistry* **50,** 4411–4426
42. Frese, C. K., Altelaarm A. F., Hennrich, M. L., Nolting, D., Zeller, M., Griep-Raming, J., Heck, A. J., and Mohammed, S. (2011) Improved peptide identification by targeted fragmentation using CID, HCD and ETD on an LTQ-Orbitrap Velos. *J. Proteome Res.* **10,** 2377–2388
43. Hart, S. R., Lau, K. W., Gaskell, S. J., and Hubbard, S. J. (2011) Distributions of ion series in ETD and CID spectra: making a comparison. *Meth. Mol. Biol.* **696,** 327–337

AQ: C AQ: D AQ: E AQ: F AQ: G AQ: H AQ: I

AUTHOR QUERIES

AUTHOR PLEASE ANSWER ALL QUERIES **1**

A—Please provide a set of revised Figs with Fig parts labeled in Caps.

B—There are 10 Figs on Web pg but you cite 11 Figs in text. Please clarify this.

C—Please provide name of Journal for reference 11.

D—We were unable to verify your reference 16 in PubMed, please confirm that it is correct or change as needed.

E—Please provide vol# for reference 18.

F—Please provide vol# for reference 26.

G—We were unable to verify your reference 36 in PubMed, please confirm that it is correct or change as needed.

H—We were unable to verify your reference 37 in PubMed, please confirm that it is correct or change as needed.

I—We were unable to verify your reference 43 in PubMed, please confirm that it is correct or change as needed.